JST

JOURNAL OF SCIENCE AND TECHNOLOGY
ISSN: 2229-8460 e-ISSN: 2600-7924

Vol. 18 No. 1 (2026) 13-22
https://publisher.uthm.edu.my/ojs/index.php/jst

Design and Development of an Autonomous Solar-Powered Artificial Beehive Acoustic Deterrent System for Human–Elephant Conflict Mitigation

Muhammad Aliff Zuhairi Ariffin[1], Khairul Anuar Mohamad[1]*, Mohamad Syahmi Nordin[2], Hairul Hafizi Hasnan[3], Ahmad Fateh Mohamad Nor[1], Rohaiza Hamdan[1], Nazirah Mohamad Abdullah[4], Nor Anija Jalaludin[5]

[1] *Faculty of Electrical and Electronic Engineering, University Tun Hussein Onn Malaysia, 86400 Parit Raja, Johor, MALAYSIA*
[2] *MT Data Driven Sendirian Berhad, Lauren Laman View 63000 Cyberjaya, Selangor, MALAYSIA*
[3] *Faculty of Creative Arts, University Malaya, Lembah Pantai, 50603 Kuala Lumpur, MALAYSIA*
[4] *Faculty of Applied Science and Technology, University Tun Hussein Onn Malaysia, 86400 Pagoh, Johor, MALAYSIA*
[5] *Faculty of Engineering Technology, University Tun Hussein Onn Malaysia 84600 Pagoh, Johor, MALAYSIA*

*Corresponding Author: khairulam@uthm.edu.my
DOI: https://doi.org/10.30880/jst.2026.18.01.002

Article Info

Received: 11 July 2025
Accepted: 13 May 2026
Available online: 30 June 2026

Keywords

Human-elephant conflict, artificial beehive, acoustic deterrent system, solar-powered system, wildlife mitigation, autonomous system, off-grid monitoring, IoT-based sensing

Abstract

This paper presents the development of a solar-powered artificial beehive system designed to mitigate human–elephant conflict, overcoming the limitations of conventional deterrent methods that lack sustainability and autonomous operation. The proposed system integrates solar energy, adaptive acoustic deterrence, and smart sensing into a unified off-grid solution for continuous field deployment. The system is powered using a 50-watt solar panel and a 12V 8Ah lead-acid battery, with an ESP32 microcontroller interfacing with passive infrared (PIR) and ultrasonic sensors to enable context-aware triggering of sound outputs. The ultrasonic sensor generates frequency responses based on object proximity, producing 200 Hz for long-range detection (above 200 cm), 250 Hz for mid-range detection (100–200 cm), and 500 Hz for close-range detection (below 100 cm). The PIR sensor immediately activates a 2000 Hz signal upon motion detection. The acoustic output is amplified using a TDA2030 module and delivered through a 15-watt horn speaker. Experimental evaluation under controlled and simulated conditions demonstrated stable system operation, with the system remaining inactive in the absence of sensor inputs and producing frequency-based acoustic outputs corresponding to detected conditions. Solar performance over five days showed consistent energy generation of more than 30 W under clear conditions, with battery voltage reached 13.17 V, indicating the capability for sustained autonomous operation. The results confirm the functional integration of sensing, control, and energy subsystems for adaptive acoustic response in off-grid environments.

1. Introduction

Human–elephant conflict (HEC) has received increasing attention due to the rising frequency of interactions between humans and elephants, driven by effective wildlife conservation initiatives and the expansion of agricultural and residential activities [1], [2]. As human settlements and agricultural land encroach upon natural habitats, elephants searching for food and water often enter populated areas, resulting in crop destruction, property damage, and occasional human fatalities. These conflicts not only threaten the livelihoods of rural communities but also endanger elephant populations, as defensive responses may involve harming or killing the animals [1].

To address these challenges, sustainable and non-lethal mitigation strategies are required to protect human safety and support wildlife conservation while maintaining ecological stability [3]. One promising approach is based on elephants' natural aversion to bees, as bee sounds are perceived as threats due to the painful nature of bee stings. This behavioural response has led to the development of artificial beehive systems that function as sound deterrents [4]. In addition, using renewable energy sources such as solar power offers significant advantages for deployment in remote and off-grid rural areas, where conventional power infrastructure is limited [5].

Despite these developments, existing deterrent systems face several technical limitations. Electric fences and other conventional methods are costly, require continuous maintenance, and may pose safety risks to both humans and elephants [6]. Many artificial beehive systems rely on static sound playback or lack smart sensing capabilities, which limits their responsiveness to real-time environmental conditions. Moreover, although solar energy has been investigated as a power source, limited work has focused on integration of adaptive sensing, proximity-based response mechanisms, and energy-autonomous operation within a unified system architecture [7].

Beehive sound deterrents have been shown to induce avoidance behaviour in elephants by emitting acoustic signals in the 200–500 Hz range to simulate natural hive activity [8], [9]. Previous studies have reported deterrence success rates of up to 88.4% when these systems are combined with physical barriers or sound-based mechanisms [10]. However, current implementations often lack adaptability, rely on fixed sound outputs or manual activation, and are not optimised for energy-constrained environments. In addition, their dependence on external power sources limits their applicability in remote areas [11].

This study presents the design and development of an autonomous solar-powered artificial beehive acoustic deterrent system that integrates adaptive sensing, acoustic response, and renewable energy into a unified platform. The system uses ultrasonic and PIR sensors for proximity and motion detection, which trigger frequency-specific acoustic outputs. The proposed system aims to provide a cost-effective and sustainable approach to supporting human–elephant conflict mitigation in rural and agricultural regions of Malaysia and Southeast Asia [12], [13], [14] by combining sensing, control, and energy subsystems into an off-grid architecture.

2. Methodology

This section describes the proposed system architecture, control logic, and hardware implementation of the proposed solar-powered artificial beehive system. The methodology focuses on the integration of sensing, signal generation, and power management to enable autonomous and frequency-specific acoustic deterrence. The system operation is designed so that the microcontroller processes sensor inputs to generate frequency-specific acoustic outputs based on predefined detection conditions.

2.1 Block Diagram of Frequency Generation System

Figure 1 shows the functional block diagram of the sound-based elephant deterrent system. The ESP32 microcontroller is the central processing unit, and it receives power from the supply unit and input signals from the sensing module. The sensing module consists of an ultrasonic sensor and a PIR sensor, which provide distance-based and motion-based detection, respectively. The control logic is implemented within the ESP32, where ultrasonic sensor readings are used to classify object proximity into three predefined ranges: >200 cm, 100–200 cm, and <100 cm. Based on this classification, the ESP32 generates corresponding output frequencies of 200 Hz, 250 Hz, and 500 Hz. The PIR sensor operates as a high-priority trigger, overriding distance-based detection and activating a 2000 Hz signal upon motion detection. The signal is generated by the ESP32 using pulse-width modulation (PWM) and transmitted to the amplifier circuit. The amplifier increases the signal amplitude to a level suitable for acoustic projection. The speaker then emits an amplified sound to simulate bee buzzing, which produces a non-lethal deterrent effect.

J. of Science and Technology Vol. 18 No. 1 (2026) p. 11-20

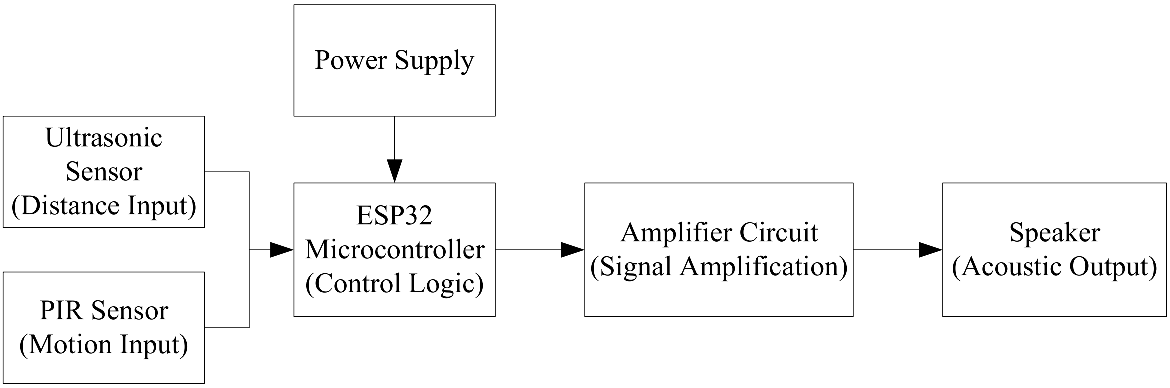

Fig. 1 *Block diagram of the sound-based elephant deterrent system*

2.2 Circuit Design using Fritzing Software

Figure 2 shows the hardware implementation of the proposed system. The system is powered by a 12V battery, which is charged from a 50W solar panel connected to a solar charge controller. This configuration enables continuous operation in off-grid environments. The ESP32 microcontroller is interfaced with an ultrasonic sensor and a PIR motion sensor. The ultrasonic sensor measures object distance using time-of-flight principles, while the PIR sensor detects changes in infrared radiation caused by motion. The ESP32 continuously samples and processes sensor data to determine the desired response. Upon detection, the ESP32 generates a frequency-specific PWM signal, which is fed into the amplifier circuit (TDA2030). The amplifier boosts the signal before it is transmitted to the speaker for acoustic output. All components are interconnected to ensure synchronised operation between sensing, signal generation, and sound output. Although the circuit layout is illustrated using Fritzing software, it represents a practical wiring configuration rather than a formal schematic.

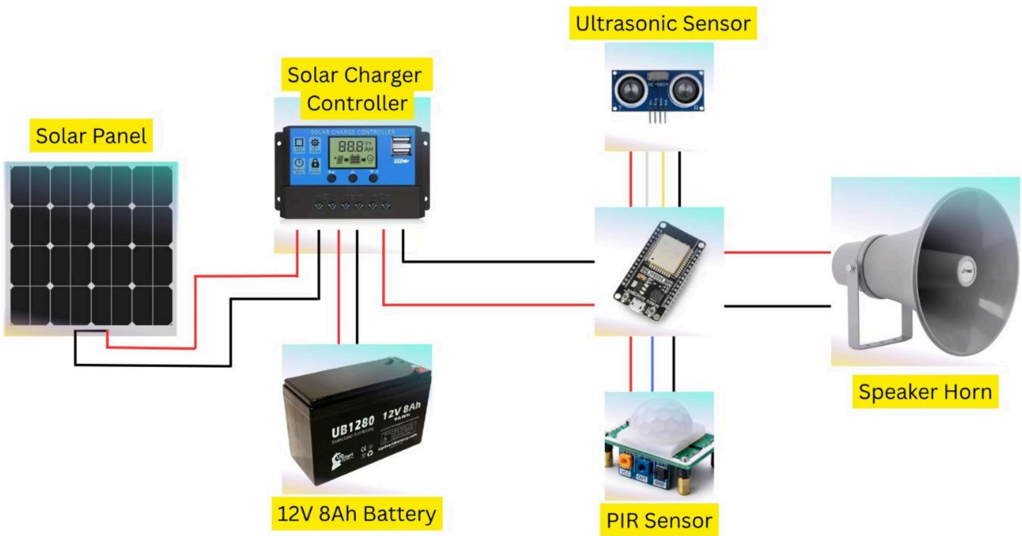

Fig. 2 *Circuit diagram of the solar-powered deterrent system*

2.3 Experimental Setup and Testing Conditions

The proposed system was evaluated under controlled and simulated conditions to assess its functional performance and operational reliability. The testing environment was designed to emulate typical detection scenarios by introducing objects at varying distances and motion conditions within a predefined range. The ultrasonic sensor was tested across three distance intervals: >200 cm, 100–200 cm, and <100 cm, while the PIR sensor was evaluated based on motion detection within its sensing field.

System responses were observed in terms of activation behaviour, frequency output consistency, and response triggering based on sensor input conditions. In addition, solar performance was monitored over five days under outdoor conditions to evaluate energy generation and battery charging characteristics. Note that the current evaluation focuses on system functionality and integration performance rather than direct field validation with elephants. The use of simulated conditions allows controlled verification of sensing accuracy, response logic, and energy autonomy prior to real-field deployment.

3. Results and Analysis

This section presents the experimental results from testing the solar-powered artificial beehive system under controlled and simulated conditions. The evaluation focuses on verifying system functionality, including sensor responsiveness, frequency generation accuracy, power performance, and operational reliability. These tests are intended to assess the feasibility of the proposed system for autonomous off-grid deployment rather than to directly quantify deterrence effectiveness. Figure 3 presents the hardware testing procedures and corresponding observations used to evaluate the integrated performance of the proposed system. Specifically, Figure 3(a) shows the validation of frequency output generated by the ESP32 microcontroller, confirming the correct implementation of the programmed pulse-width modulation (PWM) signals. Figure 3(b) shows the system response to object detection using ultrasonic and PIR sensors, highlighting the interaction between distance-based sensing and motion-triggered override mechanisms. Meanwhile, Figure 3(c) shows the sound intensity measurements at the speaker output, indicating of the acoustic signal strength after amplification, which is critical for ensuring effective sound propagation in open environments. Lastly, Figure 3(d) shows the solar photovoltaic sub-system's performance under outdoor conditions, demonstrating the system's capability to sustain energy generation for continuous operation.

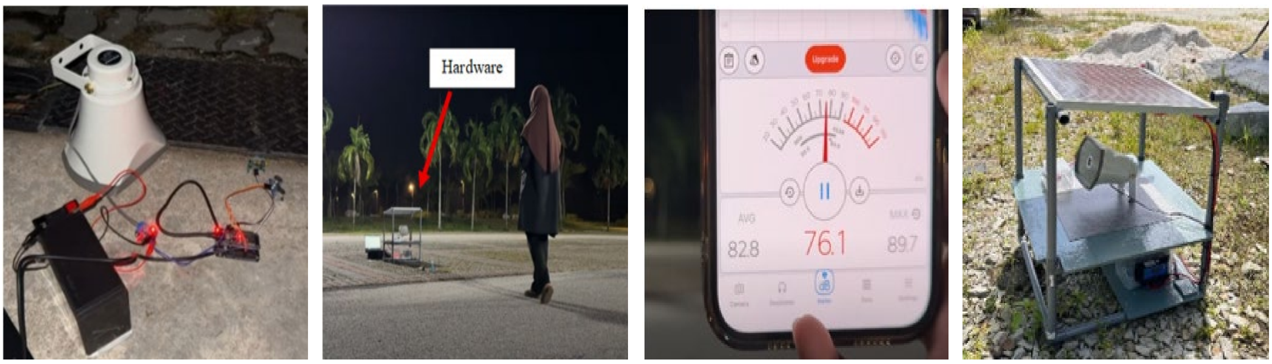

(a) (b) (c) (d)

Fig. 3 *Hardware testing results of the proposed solar-powered artificial beehive system under simulated conditions: (a) Validation of frequency output generated by the ESP32 microcontroller; (b) Object detection response using ultrasonic and PIR sensors; (c) Measurement of acoustic output intensity at the speaker; and (d) Photovoltaic system performance for off-grid power supply*

3.1 Sensor Activation and Frequency Response

Figure 4 shows the relationship between speaker output frequency and sensor input readings, with the corresponding test data summarised in Table 1. The table presents the system response under various sensing conditions, including PIR motion detection and ultrasonic distance measurements, along with their corresponding output frequencies. The results indicate that the predefined threshold-based classification (>200 cm, 100–200 cm, and <100 cm) is correctly implemented, as all tested values fall within their respective frequency categories. The results confirm that the system consistently maps object proximity to predefined acoustic responses. Specifically, distances above 200 cm trigger a 200 Hz signal, mid-range distances (100–200 cm) produce a 250 Hz signal, and close-range detection (below 100 cm) activates a higher 500 Hz signal. This behaviour demonstrates the correct implementation of the programmed distance classification algorithm on the ESP32 microcontroller.

The consistency of frequency output across multiple test cases (e.g., Test 3 and Test 4 for mid-range detection, and Test 5 and Test 7 for close-range detection) indicate stable sensor-to-response mapping. Minor variations in measured distances (e.g., 148 cm and 107 cm) did not affect the assigned frequency category, suggesting that the system is robust to small fluctuations in ultrasonic reading. In addition, the PIR sensor functions as a high-priority override mechanism, activating a 2000 Hz signal upon motion detection regardless of distance input. This prioritisation ensures rapid system response to dynamic events, which is critical in real-world scenarios involving moving animals. From a functional perspective, the increasing frequency with decreasing distance reflects an escalation-based warning strategy, in which higher-frequency signals indicate higher threat levels. This approach is consistent with previous studies indicating that elephants respond more strongly to intense or higher-frequency bee-like sounds [11], [15].

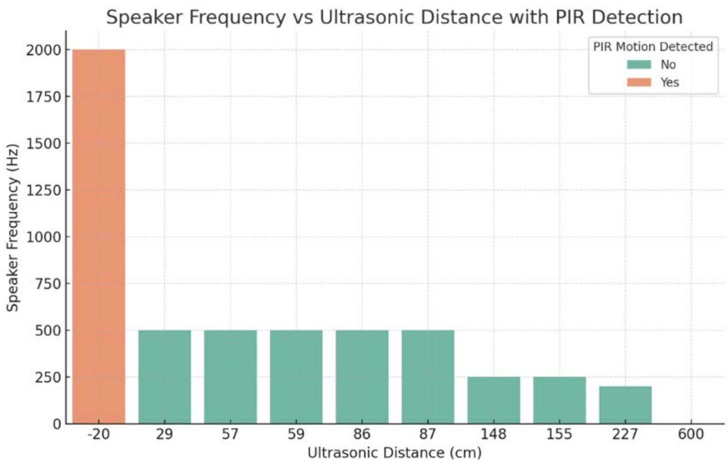

Fig. 4 *Relationship between speaker frequency and ultrasonic distance with PIR detection*

Table 1 *System response mapping between sensor inputs (ultrasonic distance and PIR motion) and speaker output frequency*

Test No.	PIR Motion Detected	Ultrasonic Distance (cm)	Speaker Frequency (Hz)	Indication
1	No	No Detection	0	No detection; speaker OFF
2	No	227	200	Far object (>2 m); low alert tone
3	No	155	250	Medium distance (1–2 m); mid alert tone
4	No	148, 107	250	Medium distance (1–2 m); consistent tone
5	No	59, 57, 29	500	Close object (<1 m); high alert tone
6	Yes	N/A	2000	Motion detected; high-priority alert
7	No	87, 86	500	Close object (<1 m); high alert tone
8	No	>600	0	Out of range; speaker OFF

3.2 Solar Panel Performance Analysis

Figure 5 shows the performance of the photovoltaic system over five consecutive days, tracking key parameters including voltage, current, power output, solar irradiation, and panel temperature between 9:00 AM and 3:00 PM daily. The voltage output showed that the system consistently maintained levels above 16 V throughout the monitoring period, which is sufficient for charging a 12 V battery. The consistent voltage output indicates stable operating conditions despite variations in solar input. Meanwhile, the current output gradually increased from morning to midday, exceeding 2.0 A during peak hours, which corresponds to increased solar irradiation and enhanced energy conversion. Power generation followed a similar trend, rising steadily from morning and reaching peak values above 30 W between 1:00 PM and 3:00 PM across all five days. Compared to the rated capacity of the 50 W solar panel, the observed output reflects typical real-world operating conditions, where factors such as temperature, solar angle, and system losses limit maximum efficiency.

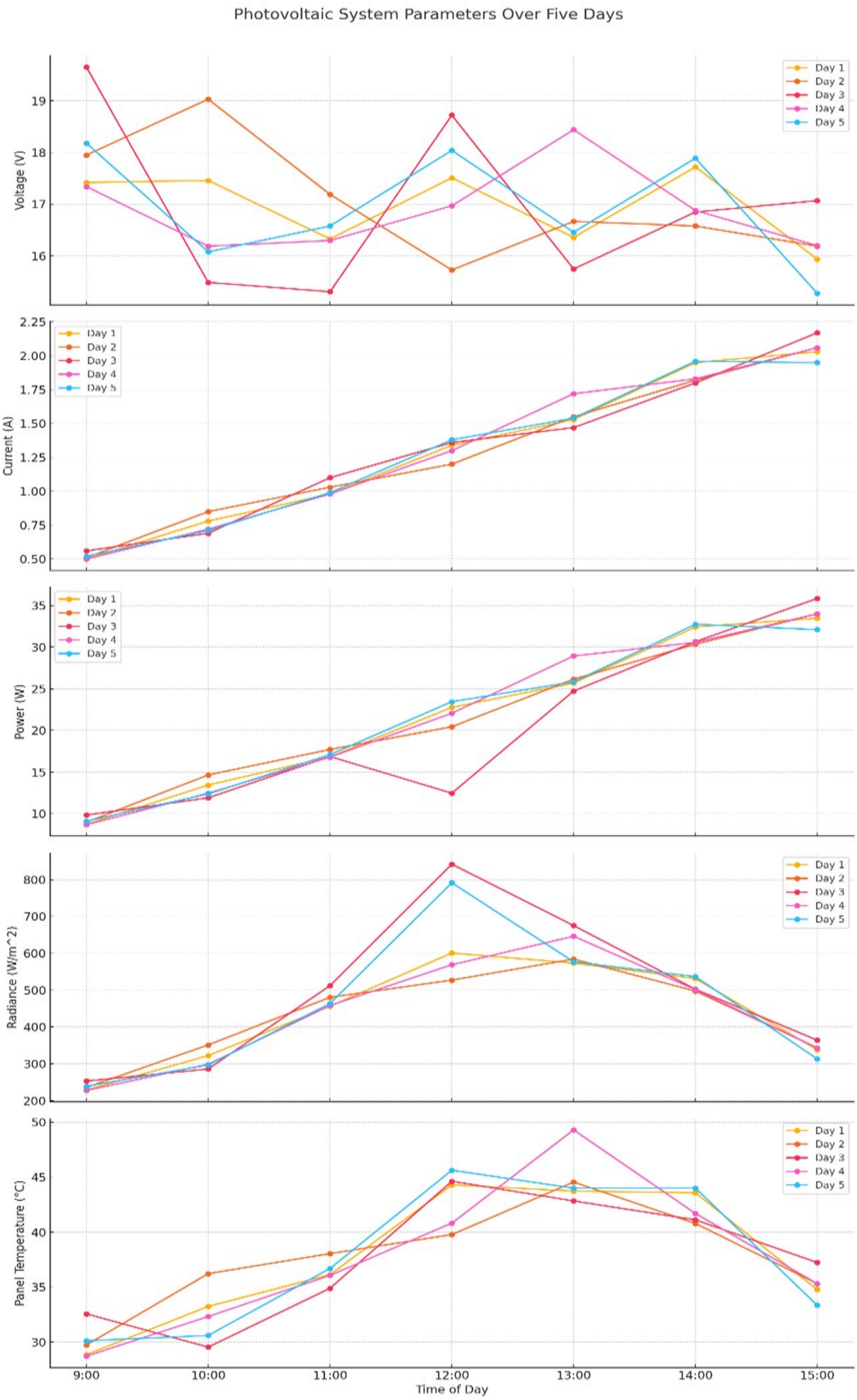

Fig. 5 *Photovoltaic system performance over five consecutive days, showing the temporal variation of voltage, current, power output, solar irradiation, and panel temperature between 9:00 AM and 3:00 PM under outdoor operating conditions*

J. of Science and Technology Vol. 18 No. 1 (2026) p. 11-20

Furthermore, solar irradiance peaked around midday at approximately 800 W/m², which aligns with the highest power output recorded. This relationship confirms the direct dependency of photovoltaic power generation on solar intensity. However, variations in power output across different days, despite comparable irradiation levels, suggest the influence of additional parameters, particularly panel temperature. Panel temperature increased steadily throughout the day, reaching peak values between 1:00 PM and 2:00 PM. Elevated temperatures are known to reduce photovoltaic efficiency, which may explain slight reductions or fluctuations in power output during peak thermal conditions. The results indicate that the photovoltaic system provides sufficient energy to support operation during daylight hours under short-term, controlled conditions.

3.3 Battery Charging Profile Without Load

Figure 6 shows the battery charging performance under no-load conditions (i.e., when no devices were active). The test was conducted over three consecutive days: 28, 29, and 30 May 2025. The results indicate that the battery voltage increased steadily from morning to the afternoon, with the highest recorded value reaching 13.17 V at 3:00 PM on the sunniest day. This result reflects the effective conversion of solar energy into stored electrical energy in the absence of system load. The gradual increase in voltage throughout the day suggests stable charging behaviour under varying solar conditions. The observed peak voltage is consistent with the expected charging range of a 12 V lead-acid battery, indicating that the charging process operates within a safe and functional range.

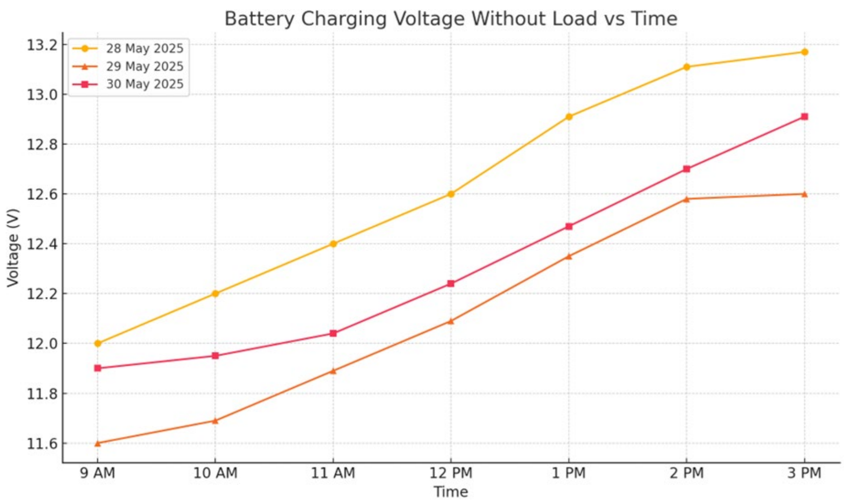

Fig. 6 *Battery voltage profile under no-load conditions over three consecutive days with the temporal variation from 9:00 AM to 3:00 PM*

3.4 Battery Charging Profile with Load

Figure 7 shows the battery charging performance during system operation under load. The data was collected over three days: 4, 5, and 6 June 2025. During this period, the battery powered the ESP32 microcontroller, sensors, and speaker system. Despite the active load, the battery voltage increased steadily throughout the day, reaching a maximum of approximately 12.9 V at 3:00 PM. Although the maximum voltage was slightly lower compared to the no-load condition, the results indicate that the photovoltaic system was still able to charge the battery while supporting continuous operation. This behaviour reflects the system's ability to simultaneously supply power to active components and store excess energy under available solar input.

A comparison across the three testing days shows that the average charging rate was approximately 0.14 V/hour on 4 June 2025, and about 0.15 V/hour on both 5 and 6 June 2025. The slightly higher charging rate observed on 5 June 2025 can be attributed to stronger solar irradiance, as indicated by the higher peak voltage on that day. A direct comparison between the no-load and load conditions indicates a reduction in charging rate from approximately 0.20 V/hour to 0.14–0.15 V/hour. The difference highlights the impact of concurrent energy consumption on battery charging performance. This comparison demonstrates the inherent trade-off between energy utilisation and storage in off-grid systems, where generated power is distributed between real-time operation and battery charging.

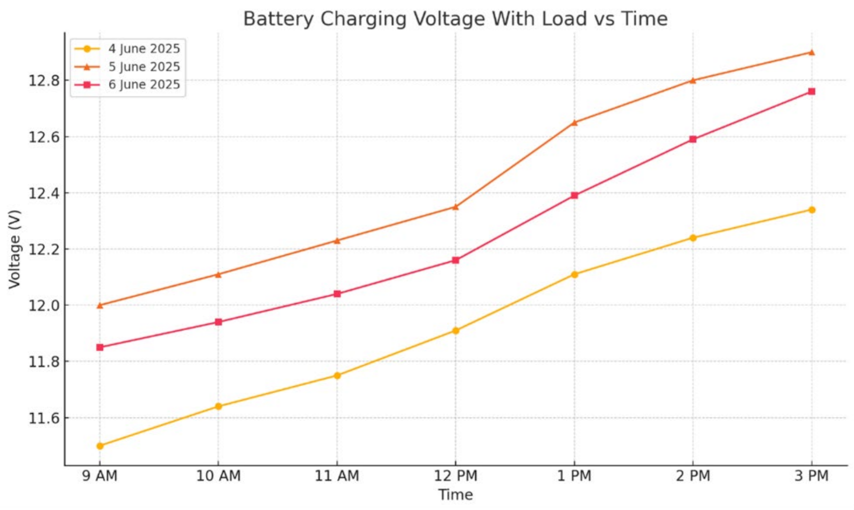

Fig. 7 *Battery voltage profile under load conditions over three consecutive days with the temporal variation from 9:00 AM to 3:00 PM*

3.5 Telegram Bot Notification Result

The Telegram bot was evaluated to assess its real-time alert detection. The ESP32 microcontroller was configured to transmit detection data, including PIR status, ultrasonic distance, and speaker output frequency, to a designated Telegram channel. Figure 8 shows the Telegram bot notifications with PIR motion, ultrasonic distance measurements, speaker frequency output, and Wi-Fi connectivity status. As shown in Figure 8, multiple system states were transmitted in real time, reflecting effective communication between the sensor and the response data. When the PIR sensor detected motion, the system generated a message indicating "PIR: Motion Detected," along with a corresponding high-frequency output of 2000 Hz, even in the absence of ultrasonic detection. In the absence of motion, the system relied on ultrasonic sensor readings, activating frequency outputs of 200 Hz, 250 Hz, or 500 Hz based on object proximity.

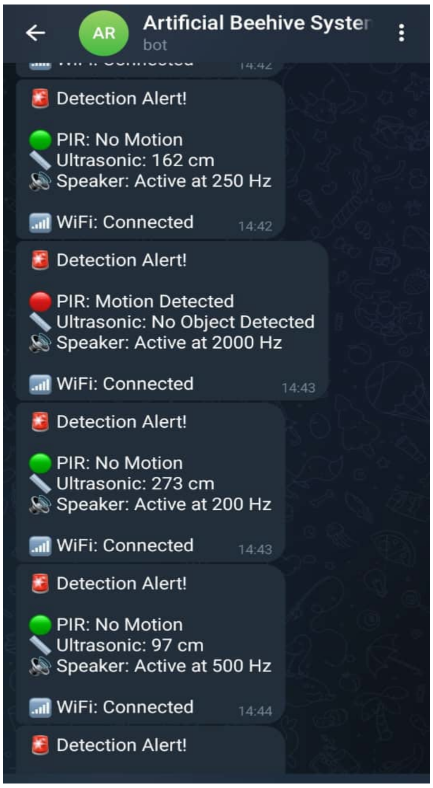

Fig. 8 *Telegram bot notifications display real-time detection with PIR motion, ultrasonic distance measurements, speaker frequency output, and Wi-Fi connectivity status*

4. Conclusion

This paper presents the development and evaluation of a solar-powered artificial beehive system designed to mitigate human–elephant conflict (HEC) in rural and off-grid environments. The system integrates sensing, control, acoustic response, and renewable energy subsystems into a unified platform capable of autonomous operation. The experimental results demonstrated that the system can generate frequency-specific acoustic responses from sensor inputs, with consistent performance across different detection scenarios. The integration of ultrasonic and PIR sensors enables prioritised and adaptive triggering, and the communication module provides real-time monitoring via Telegram notifications. In addition, solar photovoltaic performance analysis confirmed that the solar energy subsystem can support system operation during daylight hours, with stable battery charging observed under both no-load and load conditions. A comparative analysis of battery charging behaviour indicated that system load reduces the charging rate, highlighting the trade-off between energy consumption and storage in off-grid operation. Nevertheless, the system maintained continuous functionality while accumulating energy, demonstrating its feasibility for sustained deployment in energy-constrained environments.

Acknowledgement

This research was supported by Universiti Tun Hussein Onn Malaysia (UTHM) through Multi-Disciplinary Research Grant (MDR) (vot Q772).

Conflict of Interest

The authors declare that there is no conflict of interest regarding the publication of the paper.

Author Contribution

The authors confirm contribution to the paper as follows: ***study conception and design:*** *Muhammad Aliff Zuhairi Ariffin, Khairul Anuar Mohamad, Mohamad Syahmi Nordin;* ***data collection:*** *Muhammad Aliff Zuhairi Ariffin, Khairul Anuar Mohamad;* ***analysis and interpretation of results:*** *Muhammad Aliff Zuhairi Ariffin, Khairul Anuar Mohamad, Ahmad Fateh Mohamad Nor, Rohaiza Hamdan;* ***draft manuscript preparation:*** *Hairul Hafizi, Nazirah Mohamad Abdullah, Nor Anija Jalaludin. All authors reviewed the results and approved the final version of the manuscript.*

References

[1] Ortega, J., & Eggert, L. (2004b). Sukumar, R. 2003. The Living Elephants: Evolutionary Ecology, Behavior, and Conservation. Oxford University Press, New York, 478 pp. ISBN 0-19-510778-0, Journal of Mammalogy. https://doi.org/10.1644/1383960

[2] Malley, G. S., & Gorenflo, L. J. (2023). Shifts in the conflict-coexistence continuum: Exploring social-ecological determinants of human-elephant interactions. *PLoS ONE*, *18*(3), e0274155. https://doi.org/10.1371/journal.pone.0274155

[3] Kochprapa, P., Savini, C., Ngoprasert, D., Savini, T., & Gale, G. (2024). Mitigating Human-Elephant conflict in Southeast Asia. *Tropical Natural History*, *24*, 70–83. https://doi.org/10.58837/tnh.24.1.262158

[4] Basari, N., Sata, M. F. A., Mohamed, N. Z., Zamri, F. N., Samsudin, H., Shamrie, M. F., Latif, M. a. I., Yazid, S. N., & Zaidi, A. H. M. (2025). Threatening sounds as an alternative mitigation method to deter elephant: A study in Elephant Conservation Centre, Kuala Gandah, Pahang, Malaysia. Tropical Life Sciences Research, 36(1), 43–56. https://doi.org/10.21315/tlsr2025.36.1.3

[5] Karunarathne, M. (2021). Crop damage by Asian elephant (Elephas maximus) in Ekgaloya and Dewalahinda areas in Ampara District, Eastern province, Sri Lanka. Acta Fytotechnica Et Zootechnica/Acta Fytotechnica Et Zootechnica, 24(1), 47–54. https://doi.org/10.15414/afz.2021.24.01.47-54

[6] Hedges, S., & Gunaryadi, D. (2009). Reducing human–elephant conflict: do chillies help deter elephants from entering crop fields? *Oryx*, *44*(1), 139–146. https://doi.org/10.1017/s0030605309990093

[7] King, L. E., Lawrence, A., Douglas–Hamilton, I., & Vollrath, F. (2009). Beehive fence deters crop-raiding elephants. *African Journal of Ecology, 47*(2), 131–137. https://doi.org/10.1111/j.1365-2028.2009.01114.x

[8] Malek, B. a. A. (2022). Sustaining beehive-fence to reduce elephant encroachment in oil palm plantation. *Journal of Oil Palm Research, 34*(4), 715–726. https://doi.org/10.21894/jopr.2022.0050

[9] Krishnan, K. V., Krishnan, S., Raymond, B. F., & Kannan, V. (2024). Elephant Detection and Bee Frequency Deterrence System Using Artificial Intelligence. 2024 5th International Conference on Electronics and

Sustainable Communication Systems (ICESC), Coimbatore, India. https://doi.org/10.1109/icesc60852.2024.10689956

[10] Van De Water, A., King, L. E., Arkajak, R., Arkajak, J., Van Doormaal, N., Ceccarelli, V., Sluiter, L., Doornwaard, S. M., Praet, V., Owen, D., & Matteson, K. (2020). Beehive fences as a sustainable local solution to human-elephant conflict in Thailand. Conservation Science and Practice, 2(10). https://doi.org/10.1111/csp2.260

[11] Thant, Z. M., Leimgruber, P., Williams, A. C., Oo, Z. M., Røskaft, E., & May, R. (2023). Factors influencing the habitat suitability of wild Asian elephants and their implications for human–elephant conflict in Myanmar. Global Ecology and Conservation, 43, e02468. https://doi.org/10.1016/j.gecco.2023.e02468

[12] Troup, G., Heinsohn, R., King, L. E., & Edwards, K. L. (2022). Exploring seasonal variation in the faecal glucocorticoid concentrations of African elephants. Wildlife Research, 49(5), 415–427. https://doi.org/10.1071/wr21003

[13] Serenari, C., Othman, N. B., Yadav, K., Rubino, E., & Goossens, B. (2025b). Investigating blame for Human-Wildlife conflict: Reason conditions for Human-Elephant conflict in Borneo. Tropical Conservation Science, 18. https://doi.org/10.1177/19400829251375307

[14] Tsubaki, Y. (2024). Spatiotemporal patterns of human-elephant conflicts in Kota Tinggi, Malaysia, master's thesis, Tokyo Metropolitan University.

https://tokyo-metro- u.repo.nii.ac.jp/record/2001783/files/tsubaki_yuna_fulltext.pdf

[15] Akkash T. N., Sathyaraj P., Valarmathy G., Yeshwanth R. C., & Jeevesh B. (2025). Smart Drone for Surveillance and Reducing Human Elephant Conflicts. 2025 IEEE 4th International Conference for Advancement in Technology (ICONAT), 1–6, Goa, India. https://doi.org/10.1109/iconat66879.2025.11362880